JACS
JOURNAL OF THE AMERICAN CHEMICAL SOCIETY
Communication
pubs.acs.org/JACS

# Photodynamic and Photothermal Effects of Semiconducting and Metallic-Enriched Single-Walled Carbon Nanotubes

Tatsuya Murakami,*[,†] Hirotaka Nakatsuji,[‡] Mami Inada,[‡] Yoshinori Matoba,[‡] Tomokazu Umeyama,[‡,¶] Masahiko Tsujimoto,[†] Seiji Isoda,[†] Mitsuru Hashida,[†,∥] and Hiroshi Imahori*[,†,‡]

[†]Institute for Integrated Cell-Material Sciences (WPI-iCeMS), [∥]Department of Drug Delivery Research, Graduate School of Pharmaceutical Sciences, Kyoto University, Sakyo-ku, Kyoto 606-8501, Japan

[‡]Department of Molecular Engineering, Graduate School of Engineering, Kyoto University, Nishikyo-ku, Kyoto 615-8510, Japan

[¶]PRESTO, Japan Science and Technology Agency, Kawaguchi, Saitama 332-0012, Japan

Supporting Information

**ABSTRACT:** Semiconducting and metallic single-walled carbon nanotubes (s-SWNTs and m-SWNTs) were enriched by agarose gel chromatography and their photothermal and photodynamic effects were compared in $H_2O$. Under near-infrared laser irradiation, s-SWNTs generated reactive oxygen species (ROS) more than m-SWNTs, whereas m-SWNTs produced heat more efficiently than s-SWNTs. More importantly, cancer cell killing by PDE of s-SWNTs has been disclosed for the first time.

The biomedical applications of carbon nanomaterials, such as carbon nanotubes,[1−6] single-walled carbon nanohorns,[7−10] and fullerenes,[11−14] have enormous potential in current biomedical research, disease diagnosis and therapy. Among these carbon nanomaterials, single-walled carbon nanotubes (SWNTs) have remarkable optical properties of effectively absorbing near-infrared light (NIR, $\lambda$ = 650−900 nm) at their $M_{11}$ band of the metallic SWNTs and the $S_{22}$ band of the SWNTs. The NIR light is relatively harmless to our body and penetrates deep into the tissue because of minimal light absorption by hemoglobin (<650 nm) and water (>900 nm).[15] Thus recent researches on SWNT-based therapeutics have emphasized the photothermal effect (PTE) under NIR irradiation.[16−20] Photothermal tumor ablation has been suggested as a noninvasive, harmless, and highly efficient cancer therapy.[21]

In light of the modified Jablonski diagram for SWNTs,[22] besides the PTE, the photodynamic effect (PDE) should be considered because SWNTs are a mixture of metallic and semiconducting SWNTs (m- and s-SWNTs). The density of state at Fermi level of m-SWNTs is finite value ($\neq$ 0), while that of s-SWNTs is zero, implying that the excitation energy in m-SWNT is converted rapidly into heat via fast nonradiative decay and that in s-SWNTs is used for the generation of reactive oxygen species (ROS). Therefore, m- and s-SWNTs are anticipated to be advantageous for showing PTE and PDE, respectively. Kataura and co-workers have recently reported on the simple and high-yield separation of m- and s-SWNTs by utilization of agarose gel electrophoresis and chromatography.[23−25] Nevertheless, to our knowledge, the biological activities depending on m- and s-SWNTs have never been examined. Here, we report on the first comparison of the PDE and PTE of semiconducting- and metallic-enriched SWNTs in details, demonstrating that the PDE of s-SWNTs can be an additional tool for photo killing of cancer cells.

Separation of m-SWNTs and s-SWNTs was performed according to the method reported by Kataura et al.[25] Briefly, HiPco SWNTs were sonicated in 2% sodium dodecyl sulfate (SDS), and ultracentrifuged to remove bundles and impurities. The supernatant was subjected to agarose gel chromatography. In this method, s-SWNTs were adsorbed selectively to the gel. As shown in Figure 1, UV−vis-NIR spectra of flow-through

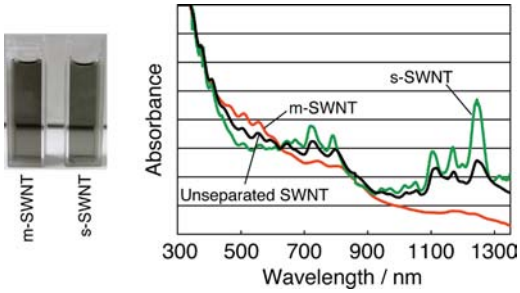


**Figure 1.** Image of m- and s-SWNT suspensions in cuvettes (left) and UV−vis-NIR spectra of m-SWNT (red), unseparated SWNT (black), and s-SWNT (green) suspensions (right).

(grayish) and adsorbed (greenish) fraction indicated that separation of m- and s-SWNTs was successful to some extent. On the basis of Raman spectroscopy analysis, the ratio of m-SWNTs: s-SWNTs in the flow-through fraction and that in the adsorbed fraction was 55:45 and 14:86, respectively (Figure S1). Moreover, few impurities were confirmed by thermogravimetric analysis (Figure S2). These metallic and semiconducting enriched fractions were used as m- and s-SWNTs in this study.

Next, the structure of our m- and s-SWNTs was characterized by atomic force microscopy (AFM) and transmission electron microscopy (TEM) measurements. Their AFM images showed that most of s-SWNTs were individually isolated, while small bundles with diameters of 1−3 nm were

**Received:** August 10, 2012
**Published:** October 19, 2012

   dx.doi.org/10.1021/ja3079972 | J. Am. Chem. Soc. 2012, 134, 17862−17865

observed for m-SWNTs. In both SWNTs, the tube length mainly ranged from 200 to 700 nm, and the length distribution displayed similar pattern (Figure S3). On the TEM specimen grids, most of both SWNTs were bundled, but by comparison of SWNTs partially isolated, there was no significant differences between m- and s-SWNTs (Figure S4).

First, the PTE of s- and m-SWNTs was compared by NIR laser irradiation at 808 nm (50 mW), which has been often used for photothermal cancer cell killing by carbon nanotubes.[17,19,20] The absorbance of both SWNT suspensions at 808 nm was adjusted to be 0.2. Under these conditions, the energy absorbed by s- and m-SWNTs is equal. After irradiation for 10 min, the temperature rise ($\Delta T$ (°C) = temperature after irradiation −23 (starting temperature)) for m-SWNT suspension was larger than that for the s-SWNT suspension (Figure 2a). With increasing the SWNT concentration, $\Delta T$ was

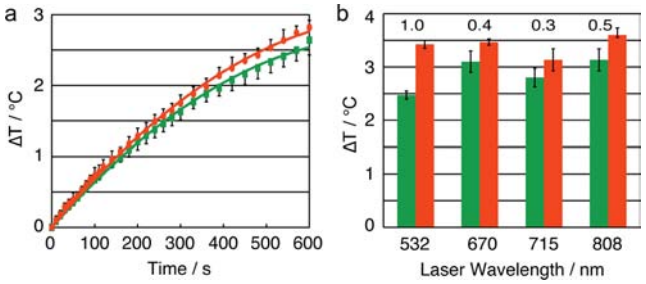


**Figure 2.** PTE of s- and m-SWNTs. (a) Time-dependent change in temperature of s- (green) and m-SWNT (red) suspension under 808-nm irradiation. (b) Effect of the laser wavelength on the difference in PTE between s- (green) and m-SWNT (red). The numbers in (b) show the difference in $\Delta T$ between s- and m-SWNTs. The concentration of SWNTs was adjusted based on the absorbance at each laser wavelength. The absorbance of SWNTs was 0.2 (a), and 0.6 (b).

increased gradually and leveled off at laser power intensities of 50 and 100 mW (Figure S5a,b). On the other hand, $\Delta T$ was almost proportional to the laser power intensity at 808 nm (Figure S5c). It should be noted that $\Delta T$ for m-SWNTs was always larger than that for s-SWNTs under these conditions. These results suggested that m-SWNTs had higher PTE than s-SWNTs.

While the two factors described above had marginal effect on difference in $\Delta T$ between s- and m-SWNTs (Figure S5), the difference in $\Delta T$ between s- and m-SWNTs was relatively influenced by the laser wavelength used (Figure 2b). The difference was in the order of 715 nm ≤ 670 nm ≤ 808 nm <5 32 nm-irradiation. These results can be rationalized by the difference in the light-absorbing ability of s- and m-SWNTs at each excitation wavelength (Figure 1). The higher light-absorbing ability of m-SWNTs than s-SWNTs at 532 nm would enhance the PTE of m-SWNT, whereas the higher light-absorbing ability of s-SWNTs than m-SWNTs at 670, 715, and 808 nm suppress the PTE of m-SWNT.

PDE results in generation of ROS, for example, singlet oxygen ($^1O_2$) and superoxide anion ($O_2^{\bullet-}$), in the presence of $O_2$. $^1O_2$ and $O_2^{\bullet-}$ are produced through energy transfer (type II mechanism) and electron transfer (type I mechanism) from the excited photosensitizers to $O_2$, respectively. Here, PDE of s-SWNTs and m-SWNTs was compared by detecting the generation of $^1O_2$ and $O_2^{\bullet-}$. Both of them were fluorescently detected after 808 nm-laser irradiation for 10 min (see Supporting Information Materials and Methods, and Figure S6). As shown in Figure 3, photoinduced generation of $^1O_2$ and

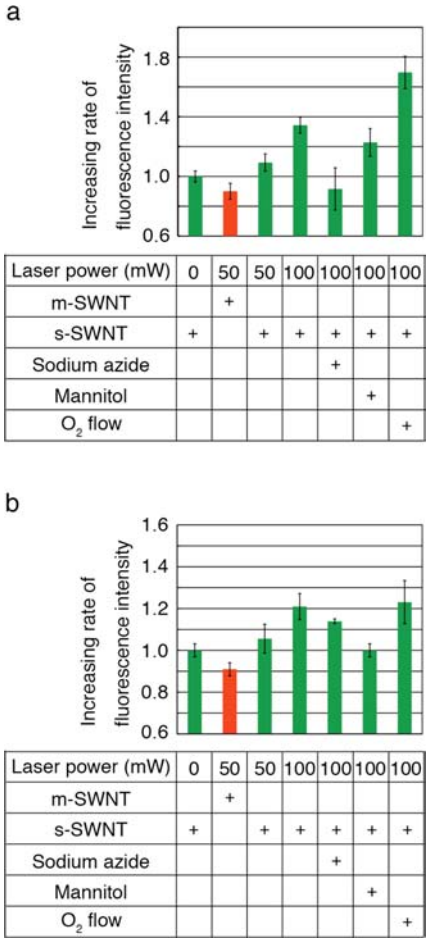


**Figure 3.** PDE of s- and m-SWNTs. $^1O_2$ (a) and $O_2^{\bullet-}$ (b) were fluorescently detected using SOSGR (Invitrogen) and Amplex UltraRed (Invitrogen), respectively. The experiments were also performed in the presence of 100 mM sodium azide (a $^1O_2$ quencher) and mannitol (a $O_2^{\bullet-}$ quencher) after $O_2$ flow in the cuvette. Data were calculated based on the integral intensity of the fluorescence spectra (see Figure S6) and normalized to the intensity for unirradiated s-SWNTs. The absorbance at 808 nm ($Abs_{808}$) of SWNTs was 0.6. Measurements were performed in triplicate ($n$ = 3).

$O_2^{\bullet-}$ was obvious only for s-SWNTs, and it was increased with increasing the laser power intensity. In addition, $^1O_2$ and $O_2^{\bullet-}$ were selectively quenched by sodium azide and mannitol, respectively,[26] which unambiguously corroborates that each fluorescent probe properly detects $^1O_2$ and $O_2^{\bullet-}$. $^1O_2$ generation was enhanced after $O_2$ flow to increase $O_2$ concentration in the dispersion, while $O_2^{\bullet-}$ generation was not. This selectivity was consistent with the conventional photochemistry of PDE.[27] Taken together, s-SWNTs were found to have much higher PDE than m-SWNTs, and to catalyze the formation of both $^1O_2$ and $O_2^{\bullet-}$.

Yamakoshi et al. reported that $O_2^{\bullet-}$ generation by water-soluble $C_{60}$ derivatives under photoirradiation is highly dependent on the concentration of a reducing agent, nicotinamide adenine dinucleotide (NADH).[28] On the other hand, Kane et al. discussed the feasibility of reduction of $O_2$ by SWNTs in the absence of reducing agents based on their redox potential and the laser wavelength (975.5 nm) used in the


dx.doi.org/10.1021/ja3079972 | J. Am. Chem. Soc. 2012, 134, 17862−17865

experiment[26] and concluded that the energy of the incident photons would be sufficient for the photoreduction of $O_2$ by SWNTs. Reduction of oxidized SWNTs has been suggested to occur by water hydroxide ions.[29,30] Thus, $O_2^{\bullet-}$ generation would also be feasible for s-SWNT aqueous dispersion without reducing agents because a shorter laser wavelength (808 nm) was used in our study.

Although m-SWNTs used in this study contained a significant amount of semiconducting components as revealed by Raman measurements (Figure S1), PDE of m-SWNTs was not detected (Figure 3). It may be possible to reconcile this apparent contradiction as follows. First, AFM measurements revealed that almost all s-SWNTs were individually isolated, while m-SWNTs were significantly bundled (Figure S3). From these data, aggregation quenching of semiconducting components, as well as energy transfer quenching of semiconducting components by metallic ones in m-SWNTs, was cited as a possible cause of the low PDE of m-SWNTs. Second, unseparated SWNTs showed a medium PDE compared with those of s-SWNTs and m-SWNTs (Figure S7), suggesting that the PDE of the SWNTs was dependent on the abundance ratio of semiconducting component in the SWNTs. Taken together, it could be concluded that enrichment of individually isolated semiconducting SWNTs enabled clear-cut detection of PDE of SWNTs under NIR irradiation.

Finally, the photo killing activity of s-SWNTs against human cancer cells, which were seeded in a 96-well plate (culture area: 0.32 $cm^2$), was examined by the 808 nm-laser irradiation (irradiation area: 0.20 $cm^2$). To reduce the cytotoxicity of deoxycholate involved in the aqueous dispersion of s-SWNTs, s-SWNTs were dialyzed against $H_2O$ after stabilized with high-density lipoprotein (HDL),[31,32] which is a naturally occurring mesoscale material capable of being bound to SWNTs.[33] The cells were irradiated for 10 min in the culture media containing the HDL-stabilized s-SWNTs, and then cultured for 24 h in a fresh medium before the assay. As shown in Figure 4, s-SWNTs markedly decreased the cell viability by 45%. Without the irradiation, the HDL-stabilized s-SWNTs did not affect the viability at all. These results clearly showed that the HDL-stabilized s-SWNTs had photo killing activity.

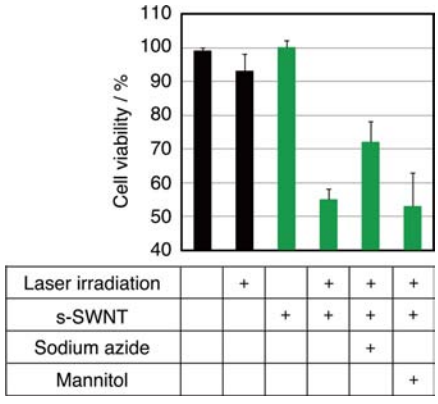


**Figure 4.** Photo killing of human lung cancer NCI-H460 cells by HDL-stabilized s-SWNTs. The cells were irradiated at 808-nm laser in the cell culture medium containing s-SWNTs ($Abs_{808}$ = 0.6) for 10 min. m-SWNTs were not subjected to the cell assay because of the severe cytotoxicity even after HDL stabilization and dialysis. The laser power intensity was increased at 800 mW to enhance the photo killing. The irradiation was also performed in the presence of both s-SWNTs and ROS quenchers. Assays were performed in triplicate ($n$ = 3).

For most photosensitizers employed in photodynamic therapy, ROS, especially $^1O_2$, play a major role in killing cancer cells.[34−37] To gain insight into the mechanism responsible for the photo killing by the HDL-stabilized s-SWNTs, the cells were irradiated in the presence of ROS quenchers, sodium azide (for $^1O_2$) or mannitol (for $O_2^{\bullet-}$, ·OH and the other free radicals). As shown in Figure 4, only sodium azide weakened the photo killing activity of s-SWNTs. It was confirmed that the presence of sodium azide had no effect on the dispersion stability of s-SWNTs in the cell culture medium (Figure S8). Therefore, the possibility of aggregation inactivation of s-SWNTs by the addition of sodium azide was excluded because aggregation of SWNTs reduces absorbance at van Hove singularities in the NIR region, leading to decrease in $^1O_2$ generation. These results supported that $^1O_2$ generated through PDE of s-SWNTs were responsible for the photo killing. On the other hand, the temperature of the cell culture medium (100 $\mu$L) containing the HDL-stabilized s-SWNTs was elevated up to 41 °C, suggesting that PTE of s-SWNTs could also be involved in the photo killing in Figure 4.[38] To our knowledge, this is the first demonstration that the PDE of SWNTs can contribute to cancer cell killing. To inquire further into the mechanism of this photo killing, for example, how the HDL-stabilized s-SWNTs interacted with the cells, is a digression from the main subject of this paper.

As reported by Gandra et al., surface functionalization of SWNTs greatly affected $^1O_2$ production under irradiation at 532 nm.[39] The degree of the surface functionalization is inversely correlated with the absorbance at van Hove singularities.[40] SWNTs used for photothermal cell killing by Kam et al. and Chakravarty et al. appear not to be heavily functionalized, based on the observation of van Hove singularities in the UV−vis-NIR spectra.[17,19] Although their experimental conditions were different from ours, PDE of SWNTs may contribute to the photoinduced cell killing which has been observed using SWNTs.

In conclusion, PDE and PTE of SWNTs have been evaluated extensively by using semiconducting- and metallic-enriched SWNTs for the first time. As expected from the density of state at Fermi level of each SWNT, semiconducting- and metallic-enriched SWNTs had higher PDE and PTE, respectively. Another important finding in this study was that semiconducting-enriched SWNTs, stabilized with HDL, caused photo killing of cancer cells through $^1O_2$ generation like the other photosensitizers. Our study provides fundamental insights for developing SWNT-based cancer therapies.

## ■ ASSOCIATED CONTENT

### Ⓢ Supporting Information

Experimental details and additional figures. This material is available free of charge via the Internet at http://pubs.acs.org.

## ■ AUTHOR INFORMATION

### Corresponding Author

murakami@icems.kyoto-u.ac.jp; imahori@scl.kyoto-u.ac.jp

### Notes

The authors declare no competing financial interest.

## ■ ACKNOWLEDGMENTS

This work was supported by WPI Initiative, MEXT, Japan. This research was also supported by a Grand-in-Aid for Scientific Research (B) (T.M.), and PRESTO, JST (T.U.).

## REFERENCES


(1) Welsher, K.; Sherlock, S. P.; Dai, H. *Proc. Natl. Acad. Sci. U.S.A.* **2011**, *108*, 8943.
(2) Liu, Z.; Tabakman, S.; Welsher, K.; Dai, H. *Nano Res.* **2009**, *1*, 85.
(3) Liu, Z.; Tabakman, S. M.; Chen, Z.; Dai, H. *Nat. Protoc.* **2009**, *4*, 1372.
(4) Kostarelos, K.; Bianco, A.; Prato, M. *Nat. Nanotechnol.* **2009**, *4*, 627.
(5) Al-Jamal, K. T.; Gherardini, L.; Bardi, G.; Nunes, A.; Guo, C.; Bussy, C.; Herrero, M. A.; Bianco, A.; Prato, M.; Kostarelos, K.; Pizzorusso, T. *Proc. Natl. Acad. Sci. U.S.A.* **2011**, *108*, 10952.
(6) Lacerda, L.; Bianco, A.; Prato, M.; Kostarelos, K. *Adv. Drug Delivery Rev.* **2006**, *58*, 1460.
(7) Zhang, M.; Murakami, T.; Ajima, K.; Tsuchida, K.; Sandanayaka, A. S. D.; Ito, O.; Iijima, S.; Yudasaka, M. *Proc. Natl. Acad. Sci. U.S.A.* **2008**, *105*, 14773.
(8) Ajima, K.; Yudasaka, M.; Murakami, T.; Maigné, A.; Shiba, K.; Iijima, S. *Mol. Pharmaceutics* **2005**, *2*, 475.
(9) Murakami, T.; Ajima, K.; Miyawaki, J.; Yudasaka, M.; Iijima, S.; Shiba, K. *Mol. Pharmaceutics* **2004**, *1*, 399.
(10) Murakami, T.; Sawada, H.; Tamura, G.; Yudasaka, M.; Iijima, S.; Tsuchida, K. *Nanomedicine (London, U.K.)* **2008**, *3*, 453.
(11) Tong, J.; Zimmerman, M. C.; Li, S.; Yi, X.; Luxenhofer, R.; Jordan, R.; Kabanov, A. V. *Biomaterials* **2011**, *32*, 3654.
(12) Fillmore, H. L.; Shultz, M. D.; Henderson, S. C.; Cooper, P.; Broaddus, W. C.; Chen, Z. J.; Shu, C.-Y.; Zhang, J.; Ge, J.; Dorn, H. C.; Corwin, F.; Hirsch, J. I.; Wilson, J.; Fatouros, P. P. *Nanomedicine (London, U.K.)* **2011**, *6*, 449.
(13) Ishida, Y.; Tanimoto, S.; Takahashi, D.; Toshima, K. *Med. Chem. Commun.* **2010**, *1*, 212.
(14) Pantarotto, D.; Tagmatarchis, N.; Bianco, A.; Prato, M. *Mini-Rev. Med. Chem.* **2004**, *4*, 805.
(15) Weissleder, R. *Nat. Biotechnol.* **2001**, *19*, 316.
(16) Burke, A.; Ding, X.; Singh, R.; Kraft, R. A.; Levi-Polyachenko, N.; Rylander, M. N.; Szot, C.; Buchanan, C.; Whitney, J.; Fisher, J.; Hatcher, H. C.; D'Agostino, J., R.; Kock, N. D.; Ajayan, P. M.; Carroll, D. L.; Akman, S.; Torti, F. M.; Torti, S. V. *Proc. Natl. Acad. Sci. U.S.A.* **2009**, *106*, 12897.
(17) Chakravarty, P.; Marches, R.; Zimmerman, N. S.; Swafford, A. D.-E.; Bajaj, P.; Musselman, I. H.; Pantano, P.; Draper, R. K.; Vitetta, E. S. *Proc. Natl. Acad. Sci. U.S.A.* **2008**, *105*, 8697.
(18) Ghosh, S.; Dutta, S.; Gomes, E.; Carroll, D.; D'Agostino, J., R.; Olson, J.; Guthold, M.; Gmeiner, W. H. *ACS Nano* **2009**, *3*, 2667.
(19) Kam, N. W. S.; O'Connell, M.; Wisdom, J. A.; Dai, H. *Proc. Natl. Acad. Sci. U.S.A.* **2005**, *102*, 11600.
(20) Moon, H. K.; Lee, S. H.; Choi, H. C. *ACS Nano* **2009**, *3*, 3707.
(21) Rai, P.; Mallidi, S.; Zheng, X.; Rahmanzadeh, R.; Mir, Y.; Elrington, S.; Khurshid, A.; Hasan, T. *Adv. Drug Delivery Rev.* **2010**, *62*, 1094.
(22) Miller, J. *J. Chem. Educ.* **1999**, *76*, 592.
(23) Tanaka, T.; Jin, H.; Miyata, Y.; Fujii, S.; Suga, H.; Naitoh, Y.; Minari, T.; Miyadera, T.; Tsukagoshi, K.; Kataura, H. *Nano Lett.* **2009**, *9*, 1497.
(24) Tanaka, T.; Jin, H.; Miyata, Y.; Kataura, H. *Appl. Phys. Lett.* **2008**, *1*, 114001.
(25) Tanaka, T.; Urabe, Y.; Nishide, D.; Kataura, H. *Appl. Phys. Express* **2009**, *2*, 125002.
(26) Joshi, A.; Punyani, S.; Bale, S. S.; Yang, H.; Borca-Tasciuc, T.; Kane, R. S. *Nat. Nanotechnol.* **2008**, *3*, 41.
(27) Macdonald, I. J.; Dougherty, T. J. *J. Porphyrins Phthalocyanines* **2001**, *5*, 105.
(28) Yamakoshi, Y.; Umezawa, N.; Ryu, A.; Arakane, K.; Miyata, N.; Goda, Y.; Masumizu, T.; Nagano, T. *J. Am. Chem. Soc.* **2003**, *125*, 12803.
(29) Zheng, M.; Rostovtsev, V. V. *J. Am. Chem. Soc.* **2006**, *128*, 7702.
(30) Zheng, M.; Diner, B. A. *J. Am. Chem. Soc.* **2004**, *126*, 15490.
(31) Murakami, T.; Tsuchida, K.; Hashida, M.; Imahori, H. *Mol. BioSyst.* **2010**, *6*, 789.
(32) Murakami, T.; Wijagkanalan, W.; Hashida, M.; Tsuchida, K. *Nanomedicine (London, U.K.)* **2010**, *5*, 867.
(33) Ham, M.-H.; Cho, J. H.; Boghossian, A. A.; Jeng, E. S.; Graff, R. A.; Heller, D. A.; Chang, A. C.; Mattis, A.; Bayburt, T. H.; Grinkova, Y. V.; Zeiger, A. S.; Van Vliet, K. J.; Hobbie, E. K.; Sligar, S. G.; Wraight, C. A.; Strano, M. S. *Nat. Chem.* **2010**, *2*, 929.
(34) Ito, T. *Photochem. Photobiol.* **1978**, *28*, 493.
(35) Valenzeno, D. P. *Photochem. Photobiol.* **1987**, *46*, 147.
(36) Weishaupt, K. R.; Gomer, C. J.; Dougherty, T. J. *Cancer Res.* **1976**, *36*, 2326.
(37) Henderson, B. W.; Dougherty, T. J. *Photochem. Photobiol.* **1992**, *55*, 145.
(38) Gerweck, L. E. *Cancer Res.* **1985**, *45*, 3408.
(39) Gandra, N.; Chiu, P. L.; Li, W.; Anderson, Y. R.; Mitra, S.; He, H.; Gao, R. *J. Phys. Chem. C* **2009**, *113*, 5182.
(40) Dyke, C. A.; Tour, J. M. *J. Phys. Chem. A* **2004**, *108*, 11151.